

2014

Adjusting magnetic nanostructures for high-performance magnetic sensors

Xiaolu Yin

University of Nebraska-Lincoln

Ralph A. Skomski

University of Nebraska-Lincoln, rskomski2@unl.edu

David J. Sellmyer

University of Nebraska-Lincoln, dsellmyer@unl.edu

Sy-Hwang Liou

University of Nebraska-Lincoln, sliou@unl.edu

Stephen E. Russek

National Institute of Standard and Technology

See next page for additional authors

Follow this and additional works at: <http://digitalcommons.unl.edu/physicsellmyer>



Part of the [Physics Commons](#)

Yin, Xiaolu; Skomski, Ralph A.; Sellmyer, David J.; Liou, Sy-Hwang; Russek, Stephen E.; Evarts, Eric R.; Moreland, John; Edelstein, A S.; Yuan, L; Yan, M L.; and Shen, J, "Adjusting magnetic nanostructures for high-performance magnetic sensors" (2014). *David Sellmyer Publications*. 259.

<http://digitalcommons.unl.edu/physicsellmyer/259>

This Article is brought to you for free and open access by the Research Papers in Physics and Astronomy at DigitalCommons@University of Nebraska - Lincoln. It has been accepted for inclusion in David Sellmyer Publications by an authorized administrator of DigitalCommons@University of Nebraska - Lincoln.

Authors

Xiaolu Yin, Ralph A. Skomski, David J. Sellmyer, Sy-Hwang Liou, Stephen E. Russek, Eric R. Evarts, John Moreland, A S. Edelstein, L Yuan, M L. Yan, and J Shen

Adjusting magnetic nanostructures for high-performance magnetic sensors

Xiaolu Yin,¹ Ralph Skomski,¹ David Sellmyer,¹ Sy-Hwang Liou,^{1,a)} Stephen E. Russek,² Eric R. Evarts,² John Moreland,² A. S. Edelstein,³ L. Yuan,⁴ M. L. Yan,⁴ and J. Shen⁴

¹*Department of Physics and Astronomy and Nebraska Center for Materials and Nanoscience, University of Nebraska, Lincoln, Nebraska 68588-0299, USA*

²*National Institute of Standard and Technology, Boulder, Colorado 80305, USA*

³*US Army Research Laboratory, Adelphi, Maryland 20783, USA*

⁴*Western Digital Corporation, Fremont, California 94539, USA*

(Presented 6 November 2013; received 24 September 2013; accepted 21 October 2013; published online 3 April 2014)

The magnetic properties of the soft ferromagnetic layer in magnetic tunnel junctions are one of key factors to determine the performance of magnetoresistance sensors. We use a three-step orthogonal annealing procedure to modify the nanostructures of the free layer in the magnetic tunnel junction to control features such as magnetization reversal, coercivity, exchange field, and tunnel magnetoresistance ratio. We present a sensor with an improved sensitivity as high as 3944%/mT. This magnetic sensor only dissipates 200 μ W of power while operating under an applied voltage of 1 V. © 2014 AIP Publishing LLC. [<http://dx.doi.org/10.1063/1.4870315>]

Approaches to improve the sensitivity of the magnetoresistive sensors based on magnetic tunnel junctions (MTJs) are to reduce sources of noise, to increase the signal, and to understand the fundamental limitations involved. Relevant properties, such as tunneling magnetoresistance ratio (TMR), coercivity (H_c), exchange coupling field (H_e), domain structures, and noise sensitively depend on the free layer structure in the MTJ. In recent years, a number of efforts to modify the magnetic tunnel junction layer structures have been discussed by several research groups.^{1–25} There are several concepts to modify the magnetic properties of the free layer in magnetic tunnel junctions such as using hard magnet or magnetic field bias,^{18,19} using an orthogonal antiferromagnetic coupling layer,^{20–22} using two-step orthogonal annealing.^{23–25}

In this study, we discuss the variation of the magnetic properties of the free layer by changing annealing conditions that are related to the performance of the magnetoresistive sensor. By optimizing the TMR ratio, H_c , H_e , domain structures and noise, we fabricate a sensor with a sensitivity as high as 3944%/mT (with a flux concentrator). This magnetic sensor only dissipates 200 μ W of power while operating under an applied voltage of 1 V.

The MTJ layer structure used in this study is 1.5 nm Ta/25 nm Ru/7 nm Ir₂₀Mn₈₀/2.2 nm Co₄₀Fe₆₀/0.85 nm Ru/2.8 nm Co₂₀Fe₆₀B₂₀/2 nm MgO/1.5 nm Co₂₀Fe₆₀B₂₀/1 nm Ta/15 nm Ru, as shown in Fig. 1(a). The Resistance Area Product (RA) of the MTJ in parallel state is about 130 k $\Omega\mu$ m². The junctions were patterned into circles with a diameter of 30 μ m (16 junctions in series) by photolithography and argon milling. The three-step orthogonal annealing procedure is shown in Fig. 1(b). The MTJ was first annealed at 350 °C in a magnetic field of 1 T field for 1 h under a vacuum of 1.33 $\times 10^{-5}$ Pascal. This ensures that the magnetic pinning direction of the reference layer is along an axis of the

circle. The second annealing process was done at 300 °C in 0.1 T for 10 h. The magnetic field direction is perpendicular (90°) to the pinning direction of the reference layer and ensures orthogonality between the free layer and the reference layer. The third annealing step was done at 300 °C for 10 h in a magnetic field of 0.1 T that forms an angle of 270° with the pinning direction. The idea is to improve the symmetry of the orthogonal property between the free layer and the pinning direction of the reference layer.

The magnetic sensor used in this study was made using an asymmetric bridge (formed by taking two dies and rotating them so that the pinned directions were opposite to each other).^{16,24,25} The sensor voltage and preamplifier bias are supplied by batteries to minimize noise. The magnetic flux concentrator (MFC) was made using a Conetic alloy which was annealed in hydrogen at 1150 °C for 20 h with cooling rate about 1 °C/min. The shape design of Magnetic Flux Concentrator was also important for the amplitude of magnification and discussed in our previous work.¹⁶ The gap between the concentrators was about 0.8 mm.

The magnetic properties of MTJ, such as magnetization reversal behavior, magnetic coercivity (H_c), exchange coupling field (H_e), and TMR ratio, are very sensitive to the annealing conditions. As shown in Fig. 2, the sample was annealed at 350 °C in a magnetic field of 1 T, which set the pinning layer direction. The TMR ratio of this sample is about 159%. The slope of the TMR loop at the zero-magnetic field is very small.

In order to improve the zero-field slope, the second annealing process was used. The sample was heated to 300 °C in a magnetic field of 0.1 T, which set the easy axis of the free layer. The second annealing process helps the magnetization in free layer to keep orthogonal with pin layer magnetization. The zero-field slope of the TMR loop (blue line in Fig. 2), which is proportional to the sensitivity of the sensor, is increased by about 8 times. The TMR ratio remains about the same (150%) after the second annealing process. However,

^{a)}Author to whom correspondence should be addressed. Electronic mail: sliou@unl.edu.

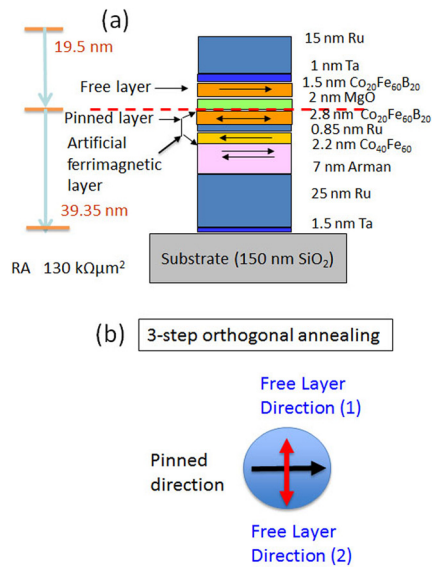


FIG. 1. Schematic MTJ structures: (a) layer sequence and (b) three-step orthogonal annealing procedures.

the coercivity H_c decreases from 1.13 mT after the first annealing to 0.87 mT after the second annealing. The exchange-coupling field H_e also decreases, from -0.33 mT after the first annealing to -0.10 mT after the second annealing.

We have tried to improve orthogonality between the free layer and the pinning direction of the reference layer by a third annealing process. We find that the TMR ratio of the sample increases to about 213% and the coercivity decreases to 0.66 mT. The exchange-coupling field also increases, to -0.35 mT after the third annealing.

The zero-field slope of TMR loop (sensitivity of the sensor, red line in Fig. 2) increases by about 13 times compared to the first annealing. The improvement of the symmetry of the MR loop of the sample may be due to the better crystal orientation of the ferromagnetic layers as well as the MgO insulator layer. The slope (dR/dH) at zero magnetic field significantly increased after third annealing. Figure 3 compares the field-dependences of the resistivity (magnetization) after the second and third annealing steps by scanning a magnetic field range of $\pm 100 \text{ mT}$. There is little difference between the parallel states

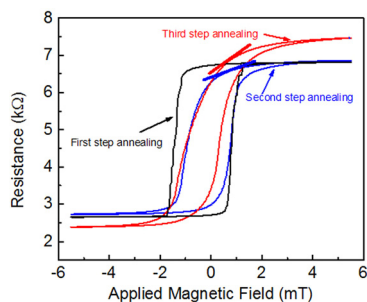


FIG. 2. TMR hysteresis loops for sample with the free layer thickness of 1.5 nm CoFeB. The black MR loop was measured after the first annealing at 350°C in a magnetic field of 1 T, which sets the pin layer direction. The blue MR loop is after the second annealing at 300°C in a magnetic field of 0.1 T, which sets the easy axis of the free layer. The red MR loop is after third annealing at 300°C in a field of 0.1, which improves the orthogonality of the free layer. The slopes of the TMR loops at zero magnetic field are marked in blue and red lines to illustrate the changing sensitivity due to annealing.

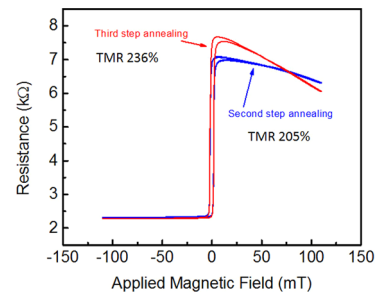


FIG. 3. TMR curves measured in fields from -100 mT to 100 mT in the easy axis direction of the reference electrode after the second annealing and after the third annealing.

(P states) after the second and third annealing steps. However, the MR loop of anti-parallel states (AP states) is more field-dependent after the third annealing step than that of the second step annealing. This indicates an additional reduction of the pinning strength after the third annealing process. One possible reason is that the AFM/FM coupling ($\text{Ir}_{20}\text{Mn}_{80}/\text{Co}_{40}\text{Fe}_{60}$) diminishes due to the diffusion of Mn at the interface forms after a high temperature and a long time (20 h) annealing. Another possible reason is that inter-diffusion of Ru occurs at the interface of the artificial antiferromagnetic coupling layers ($\text{Co}_{40}\text{Fe}_{60}/\text{Ru}/\text{Co}_{20}\text{Fe}_{60}\text{B}_{20}$).

We also observed the TMR ratios of 205% and 236% for the second and third annealing, respectively. These values are much higher than those calculated from the low-field magnetic field MR loop. We could conclude that the low-field MR loops are all minor loops, that is, the magnetization reversal of free layer is strongly coupled to the pinning layer.

Our magnetic sensor was fabricated in form of an asymmetric bridge (the Wheatstone bridge 64 MTJ junctions). Figure 4 shows the sensor voltage output as a function of the magnetic field, operating under an applied voltage of 1 V. Without magnetic flux concentrator, the sensor exhibits a fairly large magnetic hysteresis in the magnetic field range

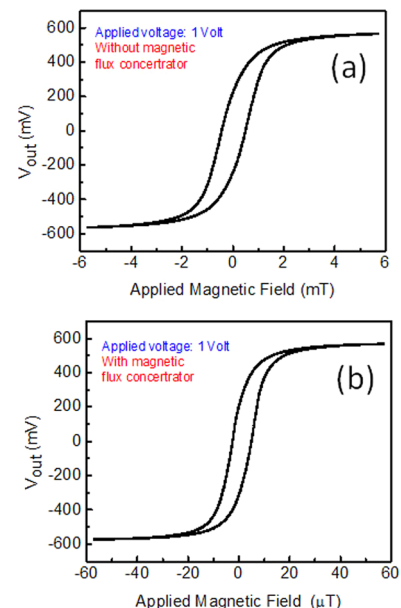


FIG. 4. Sensor output voltage (V_{out}) as a function of the magnetic field under an applied voltage of 1 V: (a) without and (b) with MFC.

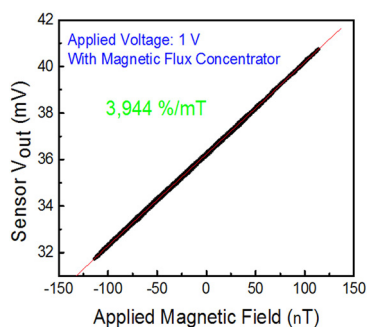


FIG. 5. Output voltage of the magnetic sensor in response to increasing and decreasing DC magnetic fields in the range of ± 125 nT. The applied voltage is 1 V, and the sensitivity of this sensor is 3944%/mT with external magnetic flux concentrator. (Note: the nearly perfect linearity of the curve.)

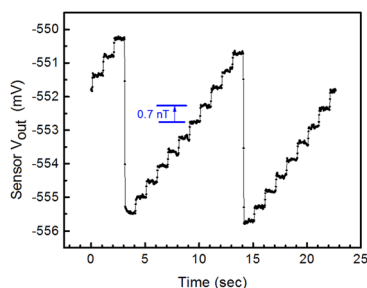


FIG. 6. Output voltage of the magnetic sensor in response to a changing DC magnetic field with 0.7 nT steps, with an applied voltage of 1 V.

of ± 6 mT. As shown in Fig. 4(b), the sensitivity of the sensor substantially improves if a magnetic flux concentrator is used. The flux concentrator was made from Conetic alloy, annealed in hydrogen at 1150 °C for 20 h. The signal of the magnetic sensor bridge with magnetic flux concentrators increases by a factor of 125. Figure 5 shows that we have achieved a sensitivity as high as 3944%/mT, with an excellent linearity between output voltage and DC magnetic field in the range of ± 125 nT.

Figure 6 shows a real-time magnetic response curve, measured under a step variation of magnetic field at 1 sec and amplitude of 0.7 nT. The applied voltage on the sensor bridge was kept at 1 V and under ambient condition. The magnetic sensor was placed inside a coil and the signal was collected by a low-noise amplifier and an A/D convertor. As shown in Fig. 6, the output voltage of the magnetic sensor clearly resolves the 0.7 nT magnetic-field steps. The output voltage of the sensor with a sensitivity of 39.4 $\mu\text{V}/\text{nT}$ responses to 0.7 nT field step with low-noise amplifier gain set at 20 is about 550 μV .

In summary, we have presented a three-step annealing method that modifies the magnetic nanostructure of the free layer in MTJ magnetic sensors. We have achieved a TMR ratio of 236% by long-time annealing at 300 °C in a magnetic

field of 0.1 T perpendicular to the hard axis of pinned layer. We show that the sensor has a very high degree of linearity in the field range of ± 100 nT and a sensitivity as high as 3944%/mT, which is the highest value has been reported so far. The sensor only dissipates 200 μW of power while operating under an applied voltage of 1 V.

This work was supported by DOD (ARO, W911NF-09-2-0039, W911NF-10-2-0099), Western Digital Corporation for the fabrication of MTJ multilayer and NSF through Nebraska MRSEC (DMR-0820521) for magnetic characterizations.

- ¹D. Wang, J. M. Daughton, Z. Qian, M. Tondra, and C. Nordman, *IEEE Trans. Magn.* **39**, 2812 (2003).
- ²M. Pannetier, C. Fermon, G. Le Goff, J. Simola, and E. Kerr, *Science* **304**, 1648 (2004).
- ³D. Wang, J. Daughton, C. Nordman, P. Eames, and J. Fink, *J. Appl. Phys.* **99**, 08H703 (2006).
- ⁴S. Ikeda, J. Hayakawa, Y. Ashizawa, Y. M. Lee, K. Miura, H. Hasegawa, M. Tsunoda, F. Matsukura, and H. Ohno, *Appl. Phys. Lett.* **93**, 082508 (2008).
- ⁵F. G. Aliev, R. Guerrero, D. Herranz, R. Villar, F. Greullet, C. Tiusan, and M. Hehn, *Appl. Phys. Lett.* **91**, 232504 (2007).
- ⁶R. C. Chaves, P. P. Freitas, B. Ocker, and W. Maass, *Appl. Phys. Lett.* **91**, 102504 (2007).
- ⁷P. P. Freitas, R. Ferreira, S. Cardoso, and F. Cardoso, *J. Phys.: Condens. Matter.* **19**, 165221 (2007).
- ⁸P. W. T. Pong, B. Schrag, A. J. Shapiro, R. D. McMichael, and W. F. Egelhoff, Jr., *J. Appl. Phys.* **105**, 07E723 (2009).
- ⁹Y. Jang, C. Nam, J. Y. Kim, B. K. Cho, Y. J. Cho, and T. W. Kim, *Appl. Phys. Lett.* **89**, 163119 (2006).
- ¹⁰A. S. Edelstein, G. A. Fischer, M. Pedersen, E. R. Nowak, S. F. Cheng, and C. A. Nordman, *J. Appl. Phys.* **99**, 08B317 (2006).
- ¹¹J. Deak, A. Jander, E. Lange, S. Mundon, D. Brownell, and L. Tran, *J. Appl. Phys.* **99**, 08B320 (2006).
- ¹²L. Yuan, S. H. Liou, and D. Wang, *Phys. Rev. B* **73**, 134403 (2006).
- ¹³L. Yuan, Y. S. Lin, D. Wang, and S. H. Liou, *IEEE Trans. Magn.* **43**, 2788 (2007).
- ¹⁴W. F. Egelhoff, Jr., V. E. Höink, J. W. Lau, W. F. Shen, B. D. Schrag, and G. Xiao, *J. Appl. Phys.* **107**, 09C705 (2010).
- ¹⁵S. H. Liou, R. Zhang, S. E. Russek, L. Yuan, S. T. Halloran, and D. P. Pappas, *J. Appl. Phys.* **103**, 07E920 (2008).
- ¹⁶S. H. Liou, D. Sellmyer, S. E. Russek, R. Heindl, F. C. S. Da Silva, J. Moreland, D. P. Pappas, L. Yuan, and J. Shen, in *proceedings of 2009 conference on IEEE Sensors* (2009), p. 1848.
- ¹⁷W. Shen, B. D. Schrag, M. J. Carter, and G. Xiao, *Appl. Phys. Lett.* **93**, 033903 (2008).
- ¹⁸W. Zhang, G. Xiao, and M. J. Carter, *Phys. Rev. B* **83**, 144416 (2011).
- ¹⁹R. C. Chaves, S. Cardoso, R. Ferreira, and P. P. Freitas, *J. Appl. Phys.* **109**, 07E506 (2011).
- ²⁰B. Negulescu, D. Lacour, F. Moutaigne, A. Gerken, J. Paul, V. Spetter, J. Marien, C. Duret, and M. Hehn, *Appl. Phys. Lett.* **95**, 112502 (2009).
- ²¹K. Fujiwara, M. Oogane, F. Kou, D. Watanabe, H. Naganuma, and Y. Ando, *J. Appl. Phys.* **50**, 013001 (2011).
- ²²K. Fujiwara, M. Oogane, S. Yokota, T. Nishikawa, H. Naganuma, and Y. Ando, *J. Appl. Phys.* **111**, 07C710 (2012).
- ²³J. Y. Chen, N. Carroll, J. F. Feng, and J. M. D. Coey, *Appl. Phys. Lett.* **101**, 262402 (2012).
- ²⁴S. H. Liou, X. Yin, S. E. Russek, R. Heindl, F. C. S. Da Silva, J. Moreland, D. P. Pappas, L. Yuan, and J. Shen, *IEEE Trans. Magn.* **47**, 3740 (2011).
- ²⁵X. Yin and S. H. Liou, in *proceedings of 2012 Conference on IEEE Sensors* (2012), p. 2090.